

Simulation of magnetization process and Faraday effect of magnetic bilayer films

Sheng Gao(高升), An Du(杜安), Lei Zhang(张磊), Tian-Guang Li(李天广), and Da-Cheng Ma(马大成)
Citation: Chin. Phys. B, 2024, 33 (**9**): 097505. DOI: 10.1088/1674-1056/ad5a76
Journal homepage: http://cpb.iphy.ac.cn; http://iopscience.iop.org/cpb

What follows is a list of articles you may be interested in

Anomalous Hall effect in ferromagnetic $LaCo_2As_2$ and ferrimagnetic $NdCo_2As_2$

Yu-Qing Huang(黄雨晴), Peng-Yu Zheng(郑鹏宇), Rui Liu(刘瑞), Xi-Tong Xu(许锡童), Zi-Yang Wu(吴紫阳), Chao Dong(董超), Jun-Feng Wang(王俊峰), Zhi-Ping Yin(殷志平), and Shuang Jia(贾爽)
Chin. Phys. B, 2023, 32 (**10**): 107502. DOI: 10.1088/1674-1056/acd925

Tuning magneto-dielectric properties of Co_2Z ferrites via Gd doping for high-frequency applications

Jian Wu(武剑), Bing Lu(卢冰), Ying Zhang(张颖), Yixin Chen(陈一鑫), Kai Sun(孙凯), Daming Chen(陈大明), Qiang Li(李强), Yingli Liu(刘颖力), and Jie Li(李颉)
Chin. Phys. B, 2023, 32 (**9**): 097501. DOI: 10.1088/1674-1056/acc3f7

Magnetic ordering induced magnetodielectric effect in $Ho_2Cu_2O_5$ and $Yb_2Cu_2O_5$

Hao Jin(金昊), Shuai Huang(黄帅), Kai-Qi Wan(万凯奇), Chang-Ming Zhu(朱长明),Hai-Ou Wang(王海欧), Kun-Peng Su(苏昆朋), and De-Xuan Huo(霍德璇)
Chin. Phys. B, 2023, 32 (**6**): 067504. DOI: 10.1088/1674-1056/ac904a

Enhancement of magnetic and dielectric properties of low temperature sintered NiCuZn ferrite by Bi_2O_3-CuO additives

Jie Li(李颉), Bing Lu(卢冰), Ying Zhang(张颖), Jian Wu(武剑), Yan Yang(杨燕), Xue-Ning Han(韩雪宁), Dan-Dan Wen(文丹丹), Zheng Liang(梁峥), and Huai-Wu Zhang(张怀武)
Chin. Phys. B, 2022, 31 (**4**): 047502. DOI: 10.1088/1674-1056/ac3399

Influence of magnetic layer thickness on $[Fe_{80}Ni_{20}–O/SiO_2]_n$ multilayer thin films

Wei Jian-Qing (魏建清), Geng Hao (耿昊), Xu Lei (徐磊), Wang Lai-Sen (王来森), Chen Yuan-Zhi (陈远志), Yue Guang-Hui (岳光辉), Peng Dong-Liang (彭栋梁)
Chin. Phys. B, 2014, 23 (**8**): 087504. DOI: 10.1088/1674-1056/23/8/087504

Simulation of magnetization process and Faraday effect of magnetic bilayer films

Sheng Gao(高升)[1], An Du(杜安)[2,3,†], Lei Zhang(张磊)[4], Tian-Guang Li(李天广)[5,6], and Da-Cheng Ma(马大成)[2]

[1] *Department of Basic and General Studies, Shenyang Institute of Science and Technology, Shenyang* 110167, *China*
[2] *College of Science, Northeastern University, Shenyang* 110819, *China*
[3] *National Frontiers Science Center for Industrial Intelligence and Systems Optimization, Northeastern University, Shenyang* 110819, *China*
[4] *Office of Academic Research, Shenyang Institute of Science and Technology, Shenyang* 110167, *China*
[5] *State Key Laboratory of Robotics, Shenyang Institute of Automation, Chinese Academy of Sciences, Shenyang* 110016, *China*
[6] *Institutes for Robotics and Intelligent Manufacturing, Chinese Academy of Sciences, Shenyang* 110016, *China*

(Received 11 March 2024; revised manuscript received 18 June 2024; accepted manuscript online 21 June 2024)

We described ferromagnetic film and bilayer films composed of two ferromagnetic layers coupled through antiferromagnetic interfacial interaction by classical Heisenberg model and simulated their magnetization state, magnetic permeability, and Faraday effect at zero and finite temperature by using the Landau–Lifshitz–Gilbert (LLG) equation. The results indicate that in a microwave field with positive circular polarization, the ferromagnetic film has one resonance peak while the bilayer film has two resonance peaks. However, the resonance peak disappears in ferromagnetic film, and only one resonance peak emerges in bilayer film in the negative circularly polarized microwave field. When the microwave field's frequency exceeds the film's resonance frequency, the Faraday rotation angle of the ferromagnetic film is the greatest, and it decreases when the thickness of the two halves of the bilayer is reduced. When the microwave field's frequency remains constant, the Faraday rotation angle fluctuates with temperature in the same manner as spontaneous magnetization does. When a DC magnetic field is applied in the direction of the anisotropic axis of the film, the Faraday rotation angle varies with the DC magnetic field and shows a similar shape of the hysteresis loop.

Keywords: magnetic bilayer films, magnetic permeability, hysteresis loop, Faraday effect, Landau–Lifshitz–Gilbert (LLG) equation

PACS: 75.70.Cn, 75.75.–c, 78.20.Ls, 77.80.Dj **DOI:** 10.1088/1674-1056/ad5a76

1. Introduction

The Faraday effect occurs when the plane of polarization of linearly polarized electromagnetic waves rotates around an axis in longitudinally magnetized materials.[1–4] We can use the Faraday effect to measure the electromagnetic properties of materials and it is also widely used in optical communication, data storage, sensors, and optical non-reciprocal devices.[1,5–8]

Nano-magnetic materials have attracted much attention in recent years and have been widely used in sensing, medicine, magnetic recording, storage devices, isolators and biotechnology.[9–15] Experimentally, Jamon *et al.* studied the micro-structured optical fibers with suspended cores covered by a silica matrix doped by $CoFe_2O_4$ nanoparticles and found that this magneto-optical material can produce relatively high Faraday rotation.[16] The Faraday rotation angle is also found to be varied with the thickness of the Cu-layer in multilayer [Co/Cu] nanofilms.[17] Kobayashi *et al.* studied transparent ferromagnetic nanogranular films composed of ferromagnetic metals and found they can generate the giant Faraday effect.[18] Mironov *et al.* constructed a constant magnet apodizing diaphragm based on the Faraday effect.[19] Li *et al.* designed an HE_{11} mode corrugated horn for microwave performance measurement of a Ka-band Faraday rotator.[20] In theory, many methods are used to study the Faraday effect. Zhu *et al.* calculated the Faraday rotation effect of 1D photonic crystals containing magnetic microcavities by transfer matrix method.[21] Using the optical pumping method, Grebenchukov *et al.* could effectively control the Faraday rotation angle of 2D material graphene.[22] Wang *et al.* studied the factors affecting the Faraday rotation angle of $Er_3Ga_5O_{12}$.[23] Nonlinear field dependence of the Faraday effect in paramagnetic neodymium gallium garnet ($Nd_3Ga_5O_{12}$) under a high magnetic field has been researched.[24] Yu *et al.* studied the Faraday effect of magnetic structure and calculated the Faraday rotation spectra.[25] Kurilkina *et al.* found the inclusion of a magnetoactive defect layer in the center of a finite dielectric three-layer periodic medium can obviously enhance the Faraday rotation angle.[26] Moreover, it can also be increased by optimizing the planar structure of the magneto-optical (MO) activity multilayer film.[27] Using first-principles density functional theory calculations, Jiang *et al.* studied the MO effects of ferromagnetic multilayers.[28] Wang *et al.* used the LLG equation to simulate the Faraday rotation angle of magnetic nanomaterials and discovered that the Faraday deflection angle could be modified by modifying the magnetic structure of the nanowire.[2] The micromagnetic method is fre-

†Corresponding author. E-mail: duan@mail.neu.edu.cn

© 2024 Chinese Physical Society and IOP Publishing Ltd

quently used to describe properly the magnetization process, AC-loss, and magnetic moment switching, and so on.[29–34]

In this study, the magnetization, permeability, and Faraday effect of magnetic bilayer films with single-ion anisotropy are studied based on the LLG equation, and the Faraday rotation angle under different magnetic structures is calculated. In Section 2, the model of magnetic bilayer films and the Faraday effect are introduced. In Section 3, the magnetization, permeability, and Faraday rotation angles of different magnetic microstructures with frequency of microwave, temperature, and external field are calculated and analyzed. In Section 4, a brief summary is given.

2. Model and method

The magnetic bilayer film is composed of two parts. A cross section of the magnetic bilayer films in the y–z plane is shown in Fig. 1. One part is the ferromagnetic layer L_1 in the z direction, and the exchange of nearest-neighbor spins is J_1, and the value of the single-ion anisotropy is D_1, and the g factor is g_1. The next part is the ferromagnetic layer L_2 with the opposite direction of spin to the first part, the exchange between the nearest-neighbor spins is J_2, the value of the single-ion anisotropy is D_2, and the g factor is g_2. J_{12} represents the exchange interaction between spins at the two interfaces, which is assumed to be antiferromagnetic.

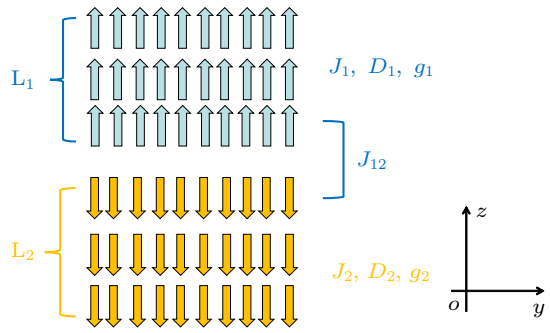


Fig. 1. Schematic diagram of the cross section of magnetic bilayer films in y–z plane.

The classical Heisenberg model is used to describe magnetic bilayer films, and the Hamiltonian is

$$H = -\sum_{ij} J_{ij}\boldsymbol{s}_i\cdot\boldsymbol{s}_j - \sum_i D_i\left(\boldsymbol{s}_i\cdot\boldsymbol{e}_i\right)^2 - \mu_0\mu_{\mathrm{B}}\sum_i g_i\boldsymbol{s}_i\cdot\boldsymbol{H}_{\mathrm{e}}. \tag{1}$$

The first part of the above formula represents the exchange interaction energy, while J_{ij} represents the exchange interaction between the spin vectors $\boldsymbol{s}_i$ and $\boldsymbol{s}_j$. The second part is the anisotropic energy, D_i is the single-ion anisotropy parameter of spin $\boldsymbol{s}_i$, $\boldsymbol{e}_i$ represents the unit vector along the anisotropic axis and it is assumed along the z direction. Spin Zeeman energy under an external magnetic field $\boldsymbol{H}_{\mathrm{e}}$ is the third term, where μ_{B} represents Bohr magneton, μ_0 represents vacuum permeability and g_i represents the g factor of each spin.

The LLG equation describes how the classical spin in the equation (1) evolves over time,[35]

$$\frac{\mathrm{d}\boldsymbol{s}_i}{\mathrm{d}t} = -\gamma\boldsymbol{s}_i\times\boldsymbol{H}_i^{\mathrm{eff}} - \alpha\gamma\boldsymbol{s}_i\times\left(\boldsymbol{s}_i\times\boldsymbol{H}_i^{\mathrm{eff}}\right). \tag{2}$$

In this context, $\gamma = g\mu_0 e/(2m)$ denotes the gyromagnetic ratio constant, while α signifies the damping constant. The effect field that is applied to the spin $\boldsymbol{s}_i$ is

$$\boldsymbol{H}_i^{\mathrm{eff}} = \frac{1}{g\mu_0\mu_{\mathrm{B}}}\left[\sum_{(i)j} J_{ij}\boldsymbol{s}_j + 2D_i(\boldsymbol{s}_i\cdot\boldsymbol{e}_i)\boldsymbol{e}_i\right] + \frac{g_i}{g}\boldsymbol{H}_{\mathrm{e}}. \tag{3}$$

Furthermore, the state of all spins in the magnetic bilayer films at any time can be obtained, and then the magnetization of the magnetic film can be calculated. The magnetization is defined as

$$M_\mu = \frac{\mu_{\mathrm{B}}}{N}\sum_{i=1}^{N} s_i^\mu\, g_i, \tag{4}$$

where μ denotes the cartesian components of x, y, and z, and N is the total number of spins.

To look into the Faraday effect exhibited by magnetic bilayer films, linearly polarizing microwaves moving in the z direction and having their polarization plane in the y–z plane are used in the system[2,36]

$$\boldsymbol{h} = \begin{pmatrix} 0 \\ 2h_0\,\mathrm{e}^{\mathrm{i}(\omega t-\beta z)} \end{pmatrix}. \tag{5}$$

It may be divided into positive circularly polarized waves and negative circularly polarized waves in the x–y plane,

$$\boldsymbol{h} = \begin{pmatrix} \mathrm{i}h_0\,\mathrm{e}^{\mathrm{i}(\omega t-\beta z)} \\ h_0\,\mathrm{e}^{\mathrm{i}(\omega t-\beta z)} \end{pmatrix} + \begin{pmatrix} -\mathrm{i}h_0\,\mathrm{e}^{\mathrm{i}(\omega t-\beta z)} \\ h_0\,\mathrm{e}^{\mathrm{i}(\omega t-\beta z)} \end{pmatrix}, \tag{6}$$

where h_0 and ω are the amplitude and frequency of the microwave, respectively. Looking against the propagation direction of the wave, the first term is a circularly polarized wave with an anticlockwise rotation of the magnetic vector, which is a microwave with positive circular polarization. The second term is a negative circularly polarized microwave with a circular polarization and a magnetic vector that rotates clockwise. Positive and negative circularly polarized microwaves within magnetic bilayer films have distinct permeability, which results in distinct propagation phase constants. The Faraday effect is caused by the microwave's polarization plane deviating from its original orientation as the propagation distance increases. The angle at which the polarization plane of a linearly polarized wave synthesized by positive and negative circular polarization rotates at position z is different from that at position $z = 0$. This angle is called the Faraday rotation angle and can be expressed as

$$\phi = \frac{1}{2}(\beta_+ - \beta_-)z = \frac{\omega}{2}\sqrt{\varepsilon_0\varepsilon_{\mathrm{r}}\mu_0}\left(\sqrt{\mu}_+ - \sqrt{\mu}_-\right), \tag{7}$$

where β_+ and β_- are microwave propagation constants for positive and negative circular polarizations, respectively, $\beta_\pm = \omega\sqrt{\varepsilon_0\varepsilon_r\mu_0\mu_\pm}$. In the given context, ε_r and ε_0 denote the vacuum dielectric constant and relative dielectric coefficient, respectively. $\mu_\pm$ signifies the relative permeability of the magnetic bilayer films when subjected to positive and negative circularly polarized fields. The following formula is the correlation with magnetic susceptibility $\chi_\pm$:

$$\mu_\pm = 1 + \chi_\pm. \tag{8}$$

Magnetic susceptibility of positive and negative circularly polarized microwave in magnetic bilayer films is[2,37,38]

$$\chi_\pm = \mp\frac{2}{h_0 T_1}\int_0^{T_1} m_x^\pm \sin\omega t\,\mathrm{d}t, \tag{9}$$

where T_1 is the period of the microwave, $T_1 = 2\pi/\omega$, and $m_x^\pm$ is the magnetization component in x direction of the bilayer films under positive and negative circularly polarized microwave at time t, which is able to be stated as

$$m_x^\pm = \frac{M_x^\pm}{v_0}, \tag{10}$$

where v_0 is the spin's volume within the bilayer films.

At finite temperature, a Gaussian random field $\boldsymbol{h}_i(t)$ should be introduced into the effective field (3) by using the fluctuation dissipation theorem,[1] which is satisfactory,

$$\langle \boldsymbol{h}_i\rangle = 0, \tag{11a}$$

$$\langle h_{i\mu}(t_1)h_{j\nu}(t_2)\rangle = 2\frac{\alpha k_\mathrm{B}T}{\gamma g\mu_0\mu_\mathrm{B}}\delta_{ij}\delta_{\mu\nu}\delta(t_1 - t_2), \tag{11b}$$

where μ and ν represent the cartesian components of x, y and z. The temperature T determines the value of the random field when the damping parameter stays constant.

In order to obtain the Faraday deflection angle of the multilayer, the volume occupied by each spin is set as $v_0 = 10^{-29}$ m^3, and the nearest-neighbor interaction between two spins is set as $J_0 = 10^{-21}$ J, which serves as the unit of energy reduction. Consequently, the exchange interactions J_1, J_2, J_{12} and the anisotropy parameters D_1 and D_2 are all expressed in units of J_0. The magnetic field is reduced in units of $H_\mathrm{k} = J_0/g\mu_0\mu_\mathrm{B}$, frequency is reduced in units of $\omega_\mathrm{k} = \gamma H_\mathrm{k}$, and the unit of time is $1/\omega_\mathrm{k}$. Temperature is reduced in units of J_0/k_B. During simulation computation, the thickness of the magnetic bilayer films is set as $L = L_1 + L_2 = 6a$, where $a = 0.22$ nm represents the separation between the spinning of nearest neighbors, periodic boundary conditions are used in the x and y directions. The film with six spin layers has four different structures, S_1, S_2, S_3 and S_4, corresponding to $L_1 = 0$ and $L_2 = 6$, $L_1 = 1$ and $L_2 = 5$, $L_1 = 2$ and $L_2 = 4$, $L_1 = 3$ and $L_2 = 3$, respectively. S_1 represents a complete ferromagnetic film, and the rest is a bilayer film formed with two ferromagnetic layers through antiferromagnetic interface interaction. In addition, we take $D_1 = D_2 = 0.5J_0$, $J_1/J_0 = J_2/J_0 = 1$, $J_{12}/J_0 = -1$, $g_1/g = 1$, $g_2/g = 1.3$, $\alpha = 0.04$, $h_0 = 0.01H_\mathrm{k}$

3. Results and discussion

3.1. The dependence of permeability and Faraday rotation angle on frequency

Figures 2(a1)–2(a4) indicate the relative permeability of bilayer films with different magnetic structures under both negatively and positively circularly polarized fields at zero temperature as a function of frequency. It is found that the magnetic permeability of the system under a circularly polarized field exhibits obvious resonance characteristics, and the resonant frequencies are all around $1.0\omega_\mathrm{k}$. According to the uniform inversion model,[39] for magnetic particles with the anisotropic value of D, the resonance frequency is $2(D/J_0)\omega_\mathrm{k}$. In the present system $D = 0.5J_0$, the resonant frequency of $1.0\omega_\mathrm{k}$ is just consistent with the uniform inversion theory. This phenomenon is similar to the resonance characteristics of the nanowires under positive and negative circularly polarized fields.[2] A minor peak in magnetic permeability occurs at a comparatively high frequency upon the introduction of the ferromagnetic layer L_1. As the thickness of the L_1 layer increases, the peak shifts in the direction of high frequency, indicating the presence of a high frequency formant induced by the L_1 layer. The effective field acting on the spins of the L_1 layer composed of anisotropic effective field and interfacial exchange field induces the second formant, its position is around $2\omega_\mathrm{k}$, and moves toward high frequency with the increase of the thickness of the L_1 layer. For the same reason, the first formant position also moves slightly towards high frequency. Under the negative circularly polarized field, as the L_1 layer appears, a small resonance occurs on the magnetic permeability at a position about frequency of $2\omega_\mathrm{k}$ [Fig. 2(a2)], as the thickness of the L_1 layer gradually increases, the resonance becomes more obvious, and the position of the formant gradually moves to the low-frequency direction until the thickness of L_1 is the same as that of L_2, and coincides with the first formant in positive circularly polarized field. Therefore, the L_2 ferromagnetic layer mainly affects the positive circularly polarized field, while L_1 mainly affects the negative circularly polarized field. When two parts are equal in thickness, the formant positions are the same. When the two layers in the film are exactly the same, the permeability is symmetric.

Figures 2(b1)–2(b4) show the variation of permeability with frequency of bilayer films with different magnetic structures under positive and negative circularly polarized fields at finite temperature. The trend of variation resembles that observed at zero temperature. As the temperature rises, the density of the random field increases, resulting in a diminishing effective field acting on spins. Consequently, the resonance frequencies exhibit a modest reduction in comparison to those observed at room temperature. The thermal fluctuation of spins also causes the apparent fluctuation of magnetic permeability.

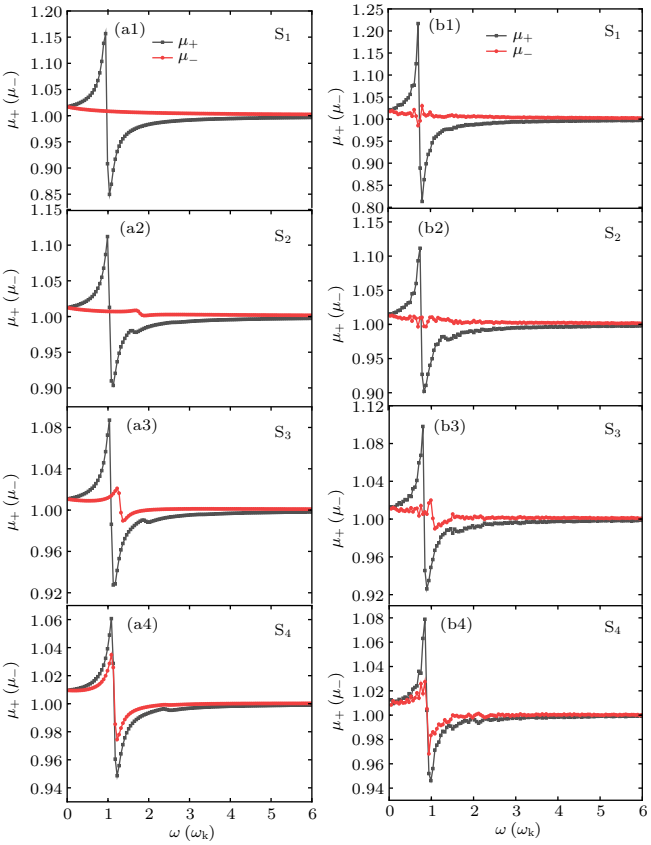


Fig. 2. The dependence of magnetic permeability on frequency of magnetic bilayer films with different magnetic structures under positive and negative circularly polarized fields. (a1)–(a4) $T = 0$, (b1)–(b4) $T = 0.6J_0/k_B$.

In the resonant region, electromagnetic waves are easily absorbed, so it is difficult to show the Faraday effect. As the frequency increases, as shown in Figs. 2(a1)–2(a4), when $\omega > 2.0\omega_k$, the permeability of the magnetic double-layer film in positive and negative circular polarization field gradually tends to be constant, at which time the Faraday effect can appear. Thus, we investigate the Faraday effect that occurs in magnetic bilayer films over a frequency range greater than $2.0\omega_k$.

Figure 3(a) depicts the Faraday rotation angle of bilayer films in a microwave field with frequency $\omega > 2.0\omega_k$. As frequency increases, the Faraday rotation angle of bilayer films with different magnetic structures decreases at zero temperature, as shown in Fig. 3(a). For a given frequency, the Faraday rotation angle of the complete ferromagnetic layer S_1 is the greatest, and it decreases as the thickness of L_1 and L_2 approaches. Because the Faraday rotation angles are caused by the propagation phase difference between positive and negative circularly polarized waves, the propagation in the L_2 layer is beneficial to the positive circularly polarized microwave and the L_2 layer is beneficial to the negative circularly polarized microwave, so they tend to counteract the rotation of the microwave polarization plane. Therefore, as the thickness of the two parts approaches, the Faraday rotation angle consequently diminishes. When the two layers in the film are exactly the same, the Faraday rotation angle is zero.

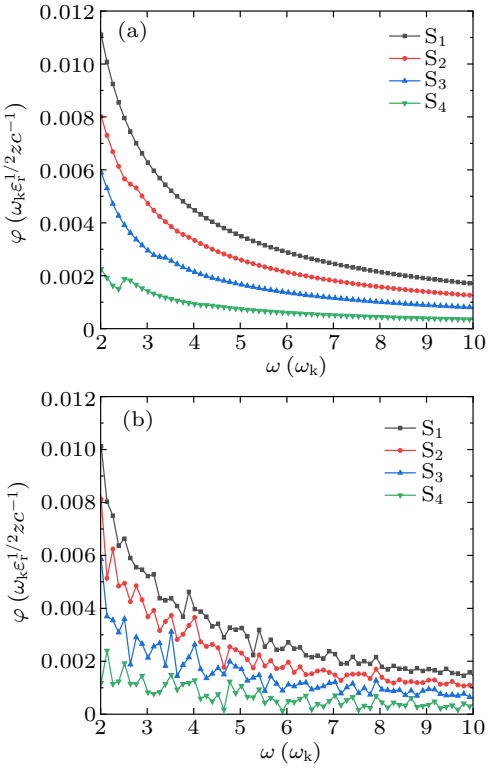


Fig. 3. The Faraday rotation angle of magnetic bilayer films with different magnetic structures as functions of microwave frequency. (a) $T = 0$, (b) $T = 0.6J_0/k_B$.

At finite temperature, as shown in Fig. 3(b), the Faraday rotation angle of bilayer films with different magnetic structures varying with frequency shows a similar trend as that at zero temperature but is smaller than that at zero temperature for a definite frequency. As the random field acting on the spin at finite temperature becomes larger, the Faraday rotation angle is disturbed randomly and shows some fluctuations.

3.2. Spontaneous magnetization and Faraday rotation angle

In order to study the effect of temperature on the AC permeability of randomly oriented magnetic bilayer films, the spontaneous magnetization behavior of four kinds of magnetic bilayer films was investigated as shown in Fig. 4(a). Figure 4(a) shows the spontaneous magnetization of bilayer films with different magnetic structures. At the same temperature, the magnetization of the complete ferromagnetic layer is the largest, and the closer the thickness of L_1 and L_2 is, the smaller the magnetization value is because the magnetizations of the bilayers cancel each other. With the increase of temperature, the density of the random field acting on spin increases, and the thermal fluctuation of spin increases, so the magnetizations of bilayer films with different magnetic structures gradually decrease with the increase of temperature, and eventually approaches zero as temperature gets to the transition temperature. It can be clearly seen that the magnetization of the mag-

netic double-layer film decreases with increasing temperature, and the transition temperature between paramagnetic and ferrimagnetic is $T = 1.7J/k_B$, and $T = 1.7J/k_B$ is the Curie temperature for the complete ferromagnetic layer (S_1). Since ferromagnetic materials become paramagnetic above the Curie temperature, we only study the relationship between permeability and temperature in the Curie temperature range. The transition temperatures of the four bilayer films with different magnetic structures are about the same, which is about $T = 1.7J_0/k_B$, which is consistent with the case of the layered quantum Heisenberg model system with different magnetic structures.[40]

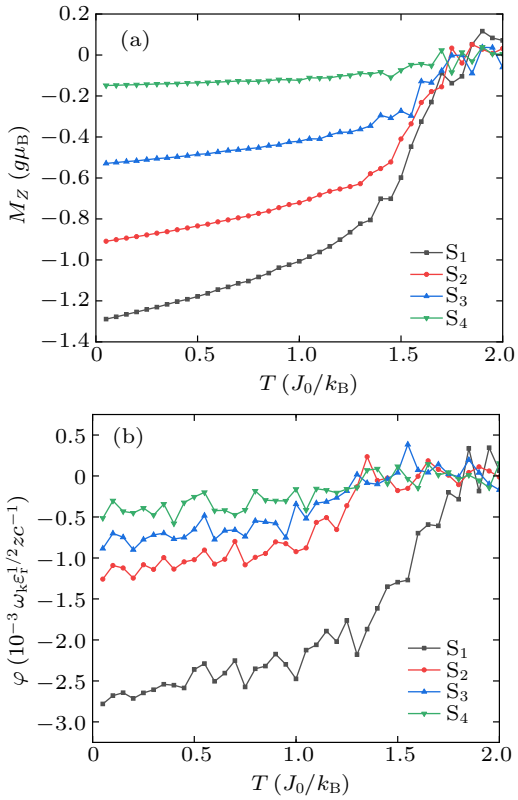


Fig. 4. (a) Temperature-dependent spontaneous magnetization of bilayer films with varied magnetic structures. (b) Faraday rotation angles of bilayer films with different magnetic structures as functions of temperature, $\omega = 6.28\omega_k$.

Figure 4(b) shows the Faraday rotation angles of bilayer films with different magnetic structures as functions of temperature. The Faraday rotation angles of films with different magnetic structures with temperature have the same trend, and it is the largest for the complete ferromagnetic layer (S_1). When the thickness of the L_1 and L_2 layers is equal, the rotation angle is the smallest. The Faraday rotation angle exhibits a progressive decrease as the temperature rises, approaching zero in proximity to the transition temperature. It can be found in Fig. 4 that the Faraday rotation angle changes with temperature and the magnetization intensity changes with temperature are similar, indicating that the spontaneous magnetization of the magnetic bilayer film is similar to the Faraday rotation angle behavior. The Faraday rotation angle is determined by the microscopic magnetic structure of the film.

3.3. Hysteresis loop and Faraday rotation angle

Figures 5(a)–5(d) show the hysteresis loops of magnetic bilayer films with different magnetic structures at zero temperature and finite temperature. As shown in Fig. 5(a) for S_1, all spins of the system at zero temperature and zero magnetic field are in the same direction. The hysteresis loop approaches a rectangular configuration, signifying that the remanence is equivalent to the magnetization at saturation. According to the uniform inversion S-W model, the spins of the system can only be reversed when the magnetic field in the opposite direction gets to the anisotropic effective field $2D/J_0(H_k)$. The coercivity being about $1.0H_k$ in the figure just conforms to the uniform inversion model.

As layer L_1 with a spin layer is covered on the L_2 layer through antiferromagnetic interaction, the hysteresis loop shows a step [Fig. 5(b)]. As the external magnetic field decreases to about $0.3H_k$, the spin of the L_1 layer begins to reverse, and magnetization changes from the value of the saturation state to the plateau of $(1.3 \times 5 - 1.0)/6(g\mu_B) = 0.92(g\mu_B)$. According to the uniform inversion theory, the anisotropic effective field of L_1 layer is $1.0H_k$, and the interfacial exchange interaction field is $-1.0H_k$. When the external field is close to $0H_k$, the spins of the L_1 layer should reverse. Near the critical field, the spin fluctuation increases, and some spins in the L_1 layer may reverse ahead, resulting in a slightly higher switching field than that of uniform reversal theory. As the magnetic field reverses and increases in the opposite direction to about $-1.0H_k$, the spins of the L_2 layer begin to reverse. After all the spins of the L_2 layer reverse, the total magnetization reaches a reverse saturation state of $-1.25g(\mu_B)$, forming a stable plateau again.

As two spin layers are covered on the L_2 layer through antiferromagnetic interfacial interaction [Fig. 5(c)], the interfacial antiferromagnetic exchange field for the overall inversion of the L_1 layer is relatively small, so the applied field decreases to about $0.1H_k$, the L_1 layer starts to reverse, and the magnetization forms a stable plateau $(1.3 \times 4 - 1 \times 2)/6(g\mu_B) = 0.53(g\mu_B)$ when the applied field decreases to about $-0.1H_k$. As the reverse magnetic field continues to increase to about $-1.1H_k$, the spins of the L_2 layer reverse, and the magnetization decreases again until the applied field gets to about $-1.2H_k$, the magnetization reaches $-1.20(g\mu_B)$, forming a second magnetization plateau. When the L_1 layer and L_2 layer are equal in thickness, as shown in Fig. 5(d), the hysteresis loop is obviously different from the previous two cases. As the external field decreases to a negative value, the spins of the L_2 layer begin to reverse first, while the spins of the L_1 layer re-

main in their original state, and the first magnetization plateau at $(1\times 3-1.3\times 3)/6=-0.15(g\mu_{\rm B})$ appears. This happens because the g factor of spin in the L_2 layer is larger than the g factor of spins in the L_1 layer, thus the spins in the L_2 layer are subjected to a larger inverse field in the same external field. As the reversing field continues to increase to about $-1.6H_{\rm k}$, the spins in the L_1 layer reverse, and gradually reach the reverse magnetization saturation state.

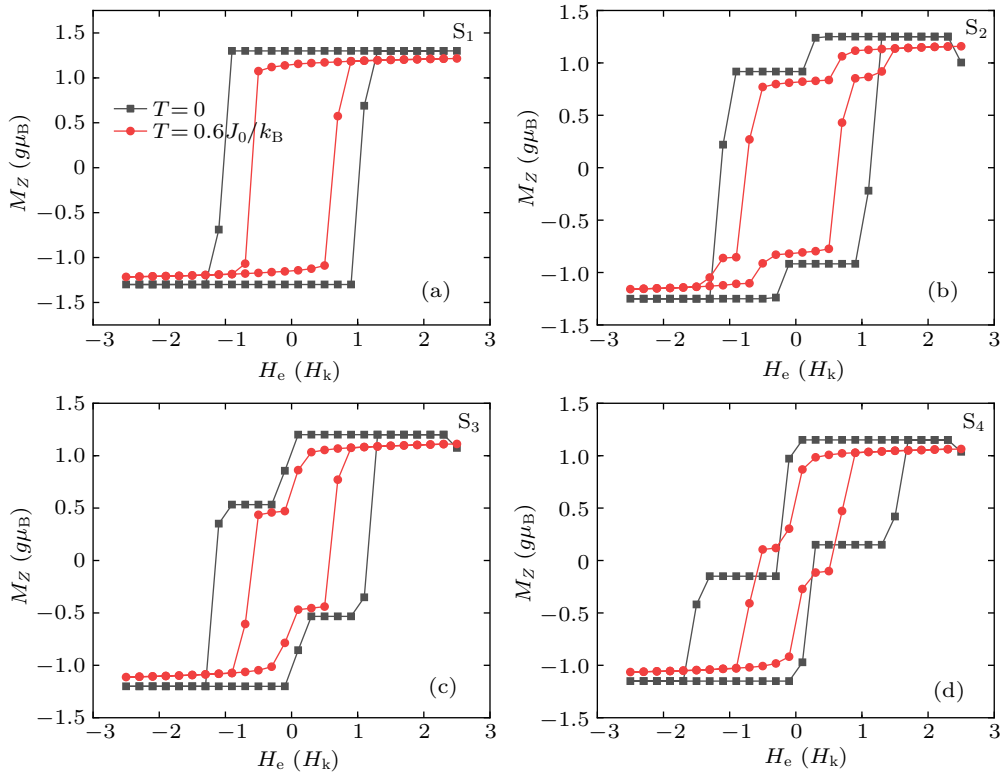


Fig. 5. Hysteresis loops of magnetic bilayer films with different magnetic structures at $T=0$ and $T=0.6J_0/k_{\rm B}$.

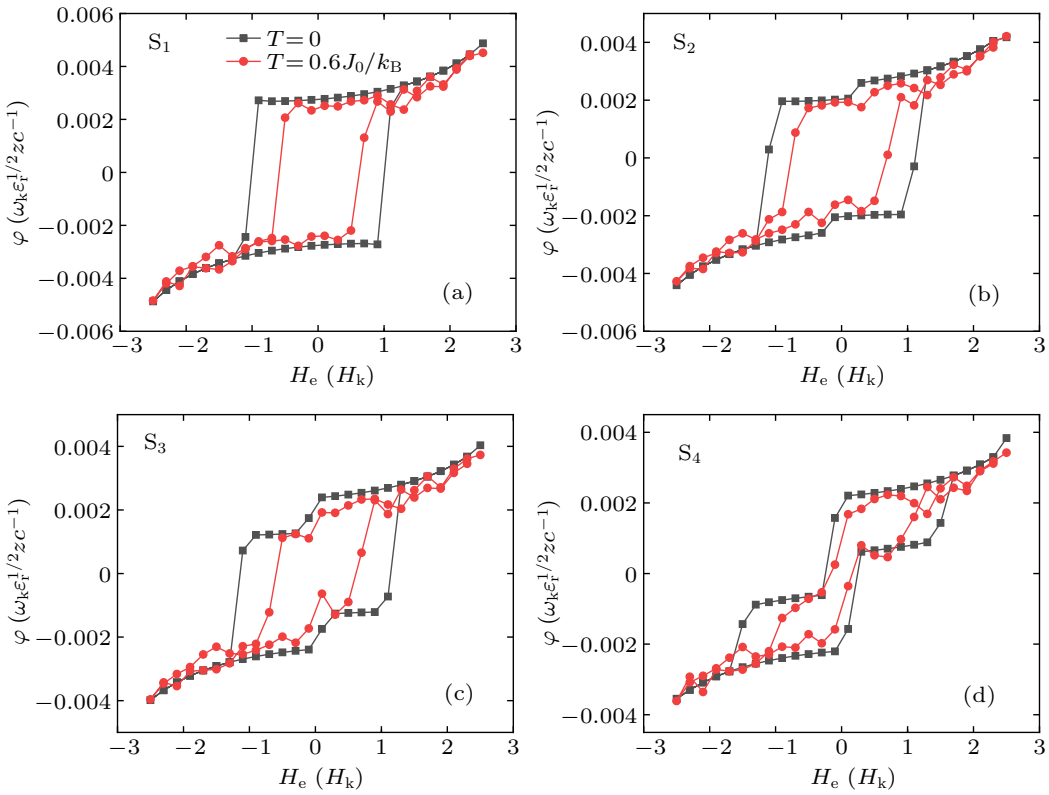


Fig. 6. Faraday rotation angles of magnetic bilayer films with different magnetic structures at $T=0$ and $T=0.6J_0/k_{\rm B}$ as functions of magnetic field.

The hysteresis behavior of the magnetic multilayer at finite temperature is similar to that at zero temperature. When the temperature increases and the random field increases, the thermal fluctuations of the spins increase, which leads to a decrease in the mean value of the spins, the remanence, and the coercivity. This result is similar to that given by Wang[2] and Wei *et al*.[41,42]

The Faraday rotation angle under different magnetic fields in Figs. 6(a)–6(d) is similar to the variation trend of the hysteresis loop given in Figs. 5(a)–5(d). At zero temperature, the Faraday rotation angle likewise exhibits a similar change when the spin direction changes from one state to another. The Faraday rotation angle exhibits a concomitant plateau when the system is in a state of stable magnetization. The Faraday rotation angle variation trend at finite temperature is almost similar to that at zero temperature; however, owing to the fluctuation of spins, the corresponding value decreases. The variation of the pulled-rotation angle with the applied DC field is similar to the behavior of the magnetization in the hysteresis loop with the applied DC field. Therefore, the Faraday rotation angle corresponds to one with the microscopic magnetic structure of the system.[2]

4. Conclusion

In this paper, the LLG equation is employed to compute the magnetization process, permeability, and Faraday rotation angle of the system under positive and negative circularly polarized fields at zero and finite temperatures, as well as to simulate the spin state of magnetic bilayer films. The variation trend of magnetic permeability with frequency is similar for magnetic bilayer films with different magnetic structures under a circularly polarized field. In the microwave field with positive circular polarization, there is a format in the ferromagnetic film, and another formant at higher frequency occurs as a ferromagnetic layer L_1 covered to the original ferromagnetic layer L_2 through antiferromagnetic exchange interaction appears, and it moves to the high frequency direction as the thickness of L_1 layer increases. In the microwave field with negative circular polarization, there is no resonance phenomenon in the ferromagnetic film, but a new formant in the higher frequency direction relative the formant in ferromagnetic film in positive circularly polarized field occurs as L_1 layer appears. As the formant migrates in the direction of low frequency, its amplitude continues to increase. The first formant in the positive circularly polarized field and the one in the negative circularly polarized field coincide when the thickness of the two ferromagnetic layers is identical. In cases where the microwave frequency is substantially higher than the resonant frequency, an increase in frequency results in a decrease in the Faraday rotation angle. The Faraday rotation angle of the ferromagnetic film is the maximum, and it is the minimum as the two parts of the film get to the same thickness. At a fixed frequency far from the resonant frequency, the Faraday rotation angle of the bilayer films with different magnetic structures changes with temperature similar to that of spontaneous magnetization. When the applied DC magnetic field is applied, the Faraday rotation angle changing with the applied DC magnetic field has the same shape as the hysteresis loop. As a result, the Faraday rotation angle corresponds to each microscopic magnetic structure individually, enabling the Faraday effect to be changed by modifying the microscopic magnetic structure of the magnetic bilayer films or applying varied DC magnetic fields.

Acknowledgement

The research was funded by the Research Program of Shenyang Institute of Science and Technology (Grant No. ZD-2024-05).

References

[1] Jin H 2013 *Physics of Ferromagnerism* (Beijing: Science Press) p. 241 (in Chinese)
[2] Wang W and Du A 2020 *J. Magn. Magn. Mater.* **511** 166591
[3] Krichevsky D M, Kalish A N, Kozhaev M A, Sylgacheva D A, Kuzmichev A N, Dagesyan S A, Achanta V G, Popova E, Keller N and Belotelov V I 2020 *Phys. Rev. B* **102** 144408
[4] Mihailovic P and Petricevic S 2021 *Sensors* **21** 6564
[5] Dadoenkova Y S, Dadoenkova N N, Lyubchanskii I L, Klos, J W and Krawczyk M 2017 *IEEE Trans. Magn.* **53** 2712278
[6] Wang H, Han J F and Lei Y Z 2021 *Opt. Commun.* **492** 126991
[7] Ghorbani-Oranj F, Abdi-Ghaleh R, Roumi B, Jamshidi-Ghaleh K, Madani A and Zhou Y G 2022 *Phys. B* **636** 413835
[8] Zhu W Q and Shan W Y 2023 *Chin. Phys. B* **32** 087802
[9] Urazhdin S, Loloee R and Pratt W P 2005 *Phys. Rev. B* **71** 100401
[10] Wang H, Dai Y Y, Gong W J, Geng D Y and Ma S 2013 *Appl. Phys. Lett.* **102** 223113
[11] Lisjak D and Mertelj A 2018 *Prog. Mater. Sci.* **95** 286
[12] Gutiérrez J, Peña A, Barandiarán J M, Pizarro J L, Hernández T, Lezama L, Insausti M and Rojo T 2000 *Phys. Rev. B* **61** 9028
[13] Tartaj P, Morales M P, González-Carreño T, Veintemillas-Verdaguer S and Serna C J 2005 *J. Magn. Magn. Mater.* **290–291** 28
[14] Jamir M, Borgohain C and Borah J P 2023 *Phys. B* **648** 414405
[15] Li H P, Pan S W, Wang Z, Xiang B and Zhu W G 2024 *Chin. Phys. B* **33** 017504
[16] Jamon D, Marin E, Neveu S, Blanc-Mignon M F and Royer F 2017 *Photonic. Nanostruct.* **27** 49
[17] Lukienko I N, Kharchenko M F, Fedorchenko A V, Kharlan I A, Tutakina O P, Stetsenko O N, Neves Cristina S and Salak A N 2020 *J. Magn. Magn. Mater.* **505** 166706
[18] Kobayashi N, Ikeda K and Arai K I 2021 *Electron. Comm. Jpn.* **141** 123
[19] Mironov E.A, Voitovich A V and Palashov O V 2013 *Opt. Commun.* **295** 170
[20] Li F, Liu G, Wang L, Balfour E. A, Wang J X, Pu Y L and Luo Y 2017 *IET Microw. Antennas Propag.* **11** 75
[21] Zhu R H, Fu S N and Peng H Y 2011 *J. Magn. Magn. Mater.* **323** 145
[22] Grebenchukov A N, Azbite S E, Zaitsev A D and Khodzitsky M K 2019 *J. Magn. Magn. Mater.* **472** 25
[23] Wang W, Zhang X J and Liu G Q 2005 *Phys. B* **365** 201
[24] Gu M, Wang W and Liu G Q 2008 *Phys. B* **403** 1

[25] Dadoenkova Y S, Dadoenkova N N, Lyubchanskii I L, Kłos J W and Krawczyk M 2017 *IEEE Trans. Magn.* **53** 2501005
[26] Kurilkina S N and Zykov A L 2005 *Opt. Spectrosc.* **98** 679
[27] Dmitriew V, Paixão F and Kawakatsu M 2013 *Opt. Lett.* **38** 1502
[28] Jiang M C and Guo G Y 2022 *Phys. Rev. B* **105** 014437
[29] Jin M H, Zheng B, Xiong L, Zhou N J and Wang L 2018 *Phys. Rev. E* **98** 022126
[30] Mondal R, Berritta M and Oppeneer P M 2016 *Phys. Rev. B* **94** 144419
[31] Gao C X, Farshchi R, Roder C, Dogan P and Brandt O 2011 *Phys. Rev. B* **83** 245323
[32] Choi M, Lee S and Kim J 2017 *IEEE Trans. Magn.* **53** 2300705
[33] Alkadour B, Mercer J I, Whitehead J P, Lierop J V and Southern J B 2016 *Phys. Rev. B* **93** 140411
[34] Ye Q Y, Wang W J, Deng C C, Chen S Y, Zhang X Y, Wang Y J, Huang Q Y and Huang Z G 2019 *Acta Phys. Sin.* **68** 107502 (in Chinese)
[35] Bajpai U and Nikolić B K 2019 *Phys. Rev. B* **99** 134409
[36] Liao S B 1988 *Ferromagnetism* (Beijing: Science Press) p. 03 (in Chinese)
[37] Picco M and Ritort F 2005 *Phys. Rev. B* **71** 100406
[38] Cao G J, Wang W and Du A 2023 *J. Magn. Magn. Mater.* **565** 170144
[39] Youssef J B and Brosseau C 2006 *Phys. Rev. B* **74** 214413
[40] Du A and Wei G Z 1994 *J. Magn. Magn. Mater.* **137** 343
[41] Song J J, Wang J, Wei D, Takahashi Y K and Hono K 2017 *IEEE Trans. Magn.* **53** 7100504
[42] Wei D, Song J J and Liu C 2016 *IEEE Trans. Magn.* **52** 7100808